Aerodynamic design for China new high-speed trains

YANG GuoWei[*], GUO DiLong, YAO ShuanBao & LIU ChengHui

LHO of Institute of Mechanics, Chinese Academy of Sciences, Beijing 100190, China

High-speed trains have very complex running environments, which contain single-train running in open air, two-trains passing by in open air, single-train running in tunnel and two-trains passing by in tunnel. When the environment wind appears, cross-wind effects must be considered. Aerodynamic design of high-speed trains mainly aims at the drag, lift, moment, impulse pressure waves, aerodynamic noise, etc. at typical running conditions. In the paper, the aerodynamic design processes of CRH380A and 380B are introduced and the aerodynamic performances of different designs are analyzed and compared. Wind tunnel experiments and running tests indicate that the new generation of high-speed trains have excellent aerodynamic performances.

aerodynamic design, CFD, wind-tunnel test, high-speed train, CRH380

1   Introduction

Since 2004, the manufacturing technologies and product lines of high-speed trains have been successively introduced into China from the different high-speed railway developed countries, which contain CRH1, CRH2, CRH3 and CRH5 four high-speed trains. In order to satisfy the requirements of China high-speed railway network, the new generation of high-speed trains of CRH380A and CRH380B, based on Japan and Germany technologies of CRH2 and CRH3, were decided to be produced, whose maximum running speed may arrive at 380 km/h.

Since the turbulence flows around the train may become more disturbances with the increase of speed, more flow energies are converted to aerodynamic drag, noise and vibrations. Many design problems which have been neglected at low train speeds are raised, such as aerodynamic noise, structural vibration due to fluid/structure interaction, impulse pressure waves as two trains are passing-by each other

and a single-train or two trains are running in tunnel, and ear discomfort of passengers inside train, etc. [1, 2]. Aerodynamic designs of the new generation of high-speed trains must consider these major limitation factors, therefore aerodynamic design for China new high-speed trains becomes one of the key techniques.

The design methods of high-speed train have currently two kinds. One is the selection from a series of design projects based on CFD evaluation and wind tunnel tests; another is the aerodynamic optimization based on the original trains. Due to the complexity of design objections and limitation conditions, so far only local and single-objective optimization for oversimplified shapes have been extensively investigated, such as, Sun et al. [3] used the CFD-based genetic algorithm to optimize the head nose shape of CRH3 to reduce aerodynamic drag, Jongsoo Lee et al. [4] and Ku et al. [5] constructed the response surface model to optimize the two-dimensional axis-symmetric nose shape for reducing micro-pressure wave, and Hyeok-bin Kwon et al. [6] optimized the train nose for minimization of tunnel sonic boom. However, the systemic design of the whole high-speed train is still the optimized selection and evalua-

*Corresponding author (email: gwyang@imech.ac.cn)

tion from many engineering experiential designs.

In the paper, the aerodynamic designs for the China new high speed trains CRH380A and 380B are briefly introduced. For the aerodynamic design of CRH380A, we mainly evaluate the aerodynamic performances for numerous design models and give the optimum selection. For the aerodynamic design of CRH380B, we mainly explore the drag deduction for the optimizations of different local structures.

2 Aerodynamic design for CRH380A

2.1 Design models

Twenty train-head models with the length of 12 m were designed by considering the numerous engineering limitation conditions, which contain the range of pilot view, equipment installation, inner space, manufacturing cost and so on. The train-head shape is determined by the geometrical design variables, such as the its length, its horizontal- and longitudinal-sectional shapes and its cross-sectional area ratio, nose and lateral cover shapes of bogie region, etc. Figure 1(a)–(e) only show their five train-head design models and Figure 1(f) gives the comparison of the longitudinal-sectional shapes of the five models. Model 5 looks like a sword and the differences of other models are mainly at nose shapes and pilot visual regions.

2.2 Aerodynamic performance

In general, the desirable China new high-speed trains should be aerodynamically stable and have lower aerodynamic forces. It is well know that the aerodynamic drag is proportional to the square of speed, while the mechanical drag is proportional to the speed. Compared with the mechanical drag, the aerodynamic drag occupies more than 80% of the total drag as the train speed exceeds 300 km/h, thus, low aerodynamic drag design is the most important issue for the new generation high-speed train design. Comparing with the aeronautical vehicles, the train length is very long and runs close to the ground; by considering the wheel/rail relation and running stability, the aerodynamic lifts of train-head and train-tail should also be lower.

The cross-wind can make the train produce lateral forces and overturn moments to influence the safe travelling, thus, the lateral forces and the overturn moments should also be lower.

First, in the open air without any cross-wind effects, the aerodynamic drag and lift coefficients were analyzed with numerical simulation for all of the twenty design models. The massive parallel hybrid grid Navier-Stokes solver with $k\omega$–SST turbulence models developed by the authors [7] was used for the numerical simulation. The calculations were carried out for these models with train-head, train-tail and one train-middle-car at a train speed of 350 km/h. Here, only the drag and lift coefficients for the above five models
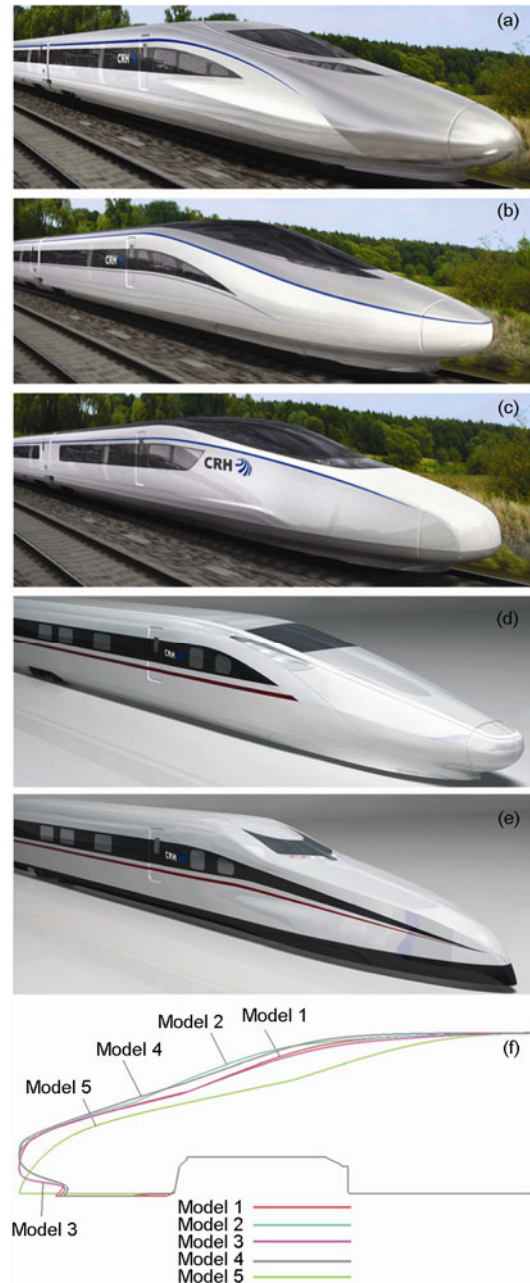

Figure 1 Five train-head models and sectional-shape comparison. (a) Model 1; (b) model 2; (c) model 2; (d) model 2; (e) model 2; (f) longitudinal sectional shapes.

are presented in Figures 2 and 3, respectively. The models of 1, 3 and 5 have the lower total drag coefficients. The lift coefficients of the train-head and train-middle cars are negative and the train-tail has positive lift, but model 1 has the lowest train-tail lift coefficient and model 5 has the highest train-tail lift coefficient. We can preliminary presume that model 1 is the best selection for the new generation of China high-speed trains.

Then, the reduced scale wind-tunnel models were designed and their tests were done at the speed of 60 m/s with yaw angles from −30° to 30°. The drag, lift and moment

coefficients, pressure distribution, aerodynamic noise, etc. were measured. Figure 4 shows the wind tunnel test model. The comparison of non-dimensional integrated aerodynamic performances for the five models is shown in Figure 5, which contains total drag, train-tail lift, train-head lateral force, train-head lateral moment and the aerodynamic far-field noise of the whole train model. It indicates that model 1 is the best in the five models. The high-speed train of CRH380A running in the railway of Beijing-Shanghai line was produced based on model 1.

Then, since the two-trains passing-by in the open air or in a tunnel and single-train running in a tunnel cannot be simulated with wind tunnel tests, and the complex running conditions can produce the impulse pressure waves and influ-

ence the structural strength of travelling train and passenger's comfort, we used numerical techniques to evaluate the amplitudes of positive and negative impulse pressure waves. The impulse waves are dependent on the speed of running trains, the shape of train-head and train-tail, train length and width, the distance between track lines, tunnel length, tunnel cross-sectional area, etc. In here, the tunnel length and cross-sectional area are taken as 2000 m and 100 m^2, respectively, the train length and the running speed are 400 m and 300 km/h, respectively. Figures 6 and 7 present the
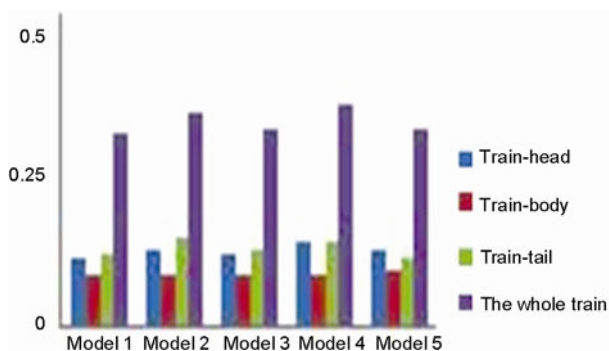

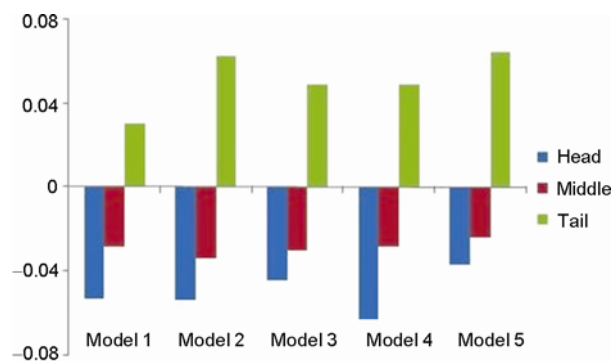**Figure 2**   Drag coefficients of the five models.

Figure 3   Lift coefficients of the five models.

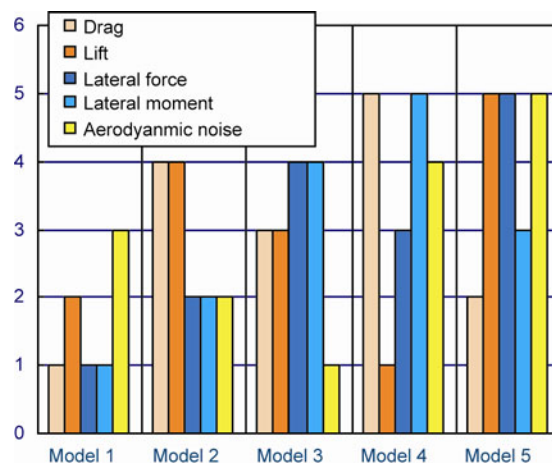**Figure 4**   Wind tunnel model.

Figure 5   Comparison of aerodynamic coefficients.
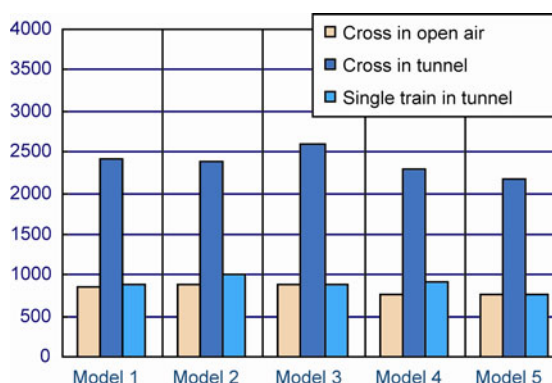

Figure 6   The maximums of positive pressure waves.
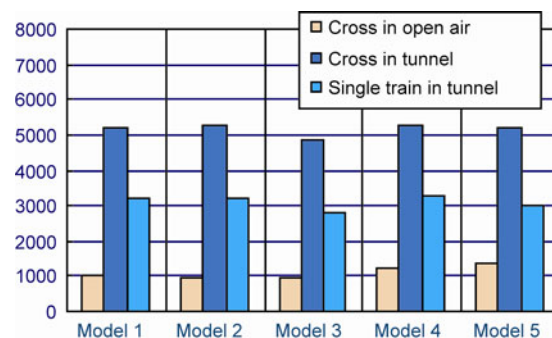

Figure 7   The minimums of absolute negative pressure waves.

comparison of the maximums of the impulse positive pressure waves and the minimums of the absolute impulse negative pressure waves for the above three complex cases, respectively. Two-trains passing-by each other in a tunnel can produce larger positive waves and negative impulse pressure waves values, which are about 2100 to 2600 Pa and −4900 to −5200 Pa, respectively. A single-train passing by in a tunnel produces the positive impulse pressure waves about 800 to 1000 Pa, and negative impulse pressure waves about −2800 to −3200 Pa. Two-trains passing by each other in open air produces the positive impulse pressure about 700 to 900 Pa, and negative impulse pressure about −900 to −1400 Pa.

The structural fatigue strength of gas tightness of the original high-speed train of CRH2 was designed based on the amplitude of impulse pressure waves of 4000 Pa and the new high-speed train of CRH380A is improved to 6000 Pa to satisfy the requirement of two-trains passing by in the tunnel.

Finally, the real high-speed train of CRH380A with eight cars (total length 200 m) at the speed 350 km/h was analyzed in the open air without cross-wind effect as shown in Figure 8. The first pantograph locates at the fourth-car, and the second pantograph at the sixth-car. The drag and lift distributions for different cars are shown in Figure 9. The fourth- and sixth-cars with pantographs have the largest drag, and the train-head and train-tail also have the larger drag. The lift coefficients from the first-car to the seventh-car are negative, however, the train-tail positive. Rela-

tively, the train-head and train-tail have the relative maximum drags.

3 Aerodynamic design for CRH380B

CRH3 was introduced into China from Siemens, which can run with the speed of 300 km/h. In order to speed it up to 350 km/h, the aerodynamic design for drag deduction was mainly concerned.

3.1 Aerodynamic drag distribution of CRH3

First, the aerodynamic drag distributions of the original CRH3 train with eight cars (total length 200 m) were calculated at the 350 km/h in the open air without any cross-wind effects. The train model for calculation is shown in Figure 10, which contains the complex bogies, pantographs and their covers, joint parts between two cars, ventilation covers, etc. The aerodynamic drag distribution from the train nose to tail along the longitudinal direction is given in Figure 11. It indicates that the drag contributions were produced mainly from train-head and train-tail, joint parts between two cars, two pantographs, and ventilation covers. For drag deduction optimization, these structures should be modified.

The percentage ratio of each car to total drag of the train is shown in Figure 12. The aerodynamic drag of train-head and train-tail occupies 31.5% of the total drag, 33.8% of the total drag for the second- and seventh-cars with two pantographs, and 34.7% for the other four cars. The contributions to the total drag of all the joint parts between two cars are presented in Figure 13. The drag sum of all joint parts is about 19% of the total drag. The first- and second-joint parts produce a much larger aerodynamic drag than other parts. The drag distributions of bogies and their installation regions are shown in Figure 14, whose sum contributes 27.4% to the total drag. Bogies drags are smaller than those of their installation regions. The first installation region of bogie has the maximum drag contribution to the total drag.

Figure 8   CRH380A model with eight-cars.
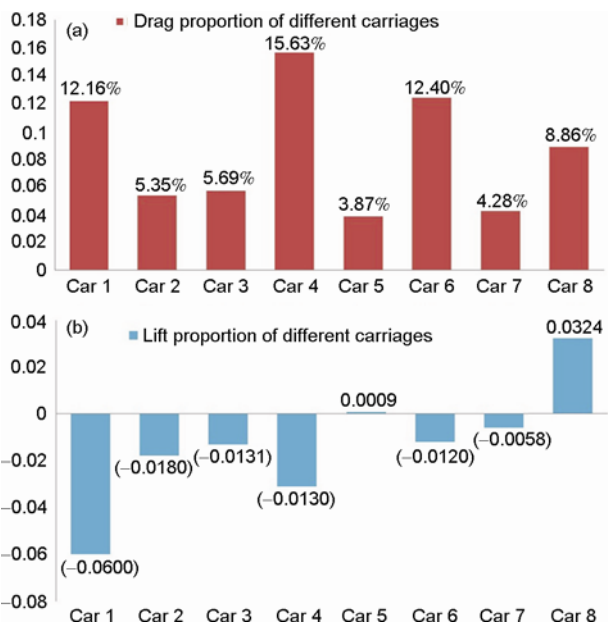

Figure 9   Aerodynamic drag and lift coefficient distributions. (a) Aerodynamic drag coefficient distribution; (b) aerodynamic lift coefficient distribution.
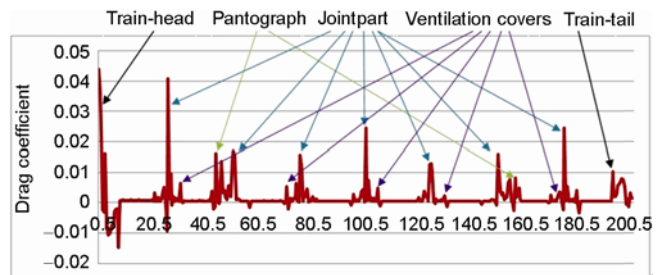

Figure 10   CRH3 model with eight cars.

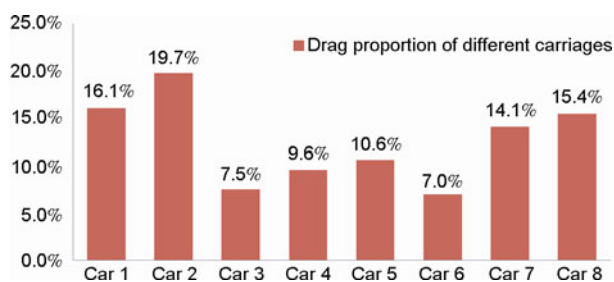**Figure 11**   Aerodynamic drag distributions along longitudinal direction (Δl=0.5 m).

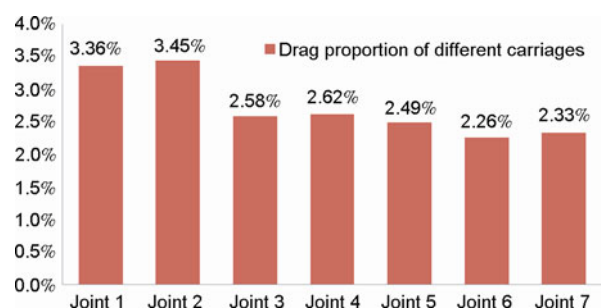**Figure 12**   Aerodynamic drag percentage ratios of different cars.

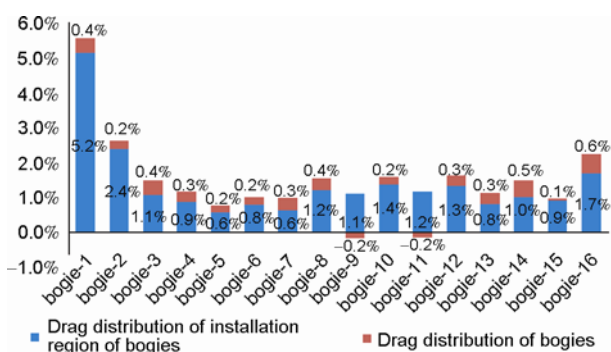**Figure 13**   Aerodynamic drag percentage ratios of different joint parts.

Figure 14   Drag percentage ratios of bogies and their installation regions.

We also evaluated the drag distributions of other parts, in which the drag of two pantographs and their covers is about 12% of the total drag, and all ventilation covers is about 7.6% of the total drag of the train. From these analyses, the aerodynamic drag distributions of all parts of the train are known, thus the drag deduction should be optimized for those parts with larger drags.

3.2   Local drag deduction design of CRH3

Through the above analyses, with the train-head and train-tail, pantographs and bogies unchangeable, the following structures are suggested to be optimized: (1) Add outer joint parts between cars as shown in Figure 15(a); (2) Modify the streamline ventilation covers as shown in Figure 15(b); (3) Modify the streamline pantograph covers as shown in Figure 15(c); (4) Enwrap the first bogie and add the skirts for other bogies as shown in Figure 15(d).
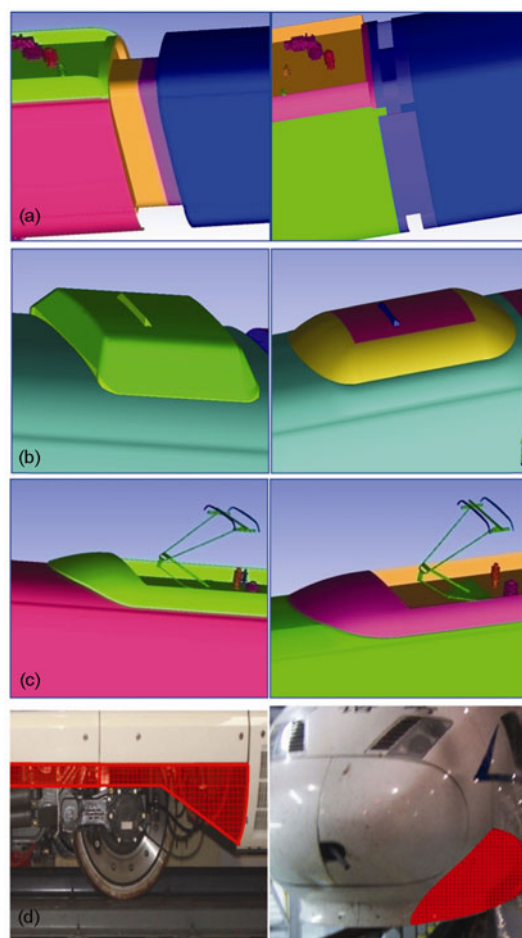

Figure 15   Local modification parts of CRH3. (a) Joint part between two cars; (b) ventilation cover; (c) pantograph cover; (d) region of bogies.

3.3   Wind tunnel tests for local modified model

Under the wind speed of 60 m/h and with 1:8 reduced scale models with three cars, the wind tunnel tests were done to check the drag deduction effects for different optimization structures. The effects of drag deduction are shown in Table 1. All local structural modifications are benefit for the aerodynamic drag deduction and the integrated optimization model 8 can reduce the total aerodynamic drag of 8.9%.

3.4   Aerodynamic performance of CRH380B

After the above wind tunnel tests, the optimized local structures were obtained for the model of three cars. We need further to know the effect of drag reduction for the real running train with eight cars. Numerical simulations were again used for the evaluation of aerodynamic performance for the optimized train. The comparison of aerodynamic drag distributions along the longitudinal direction is given in Figure 16. Local drag deductions are obvious in the optimization regions. Figure 17 shows the comparison of drag distributions for eight cars. The drag deductions for different cars present an anti-symmetric change, namely, the drag
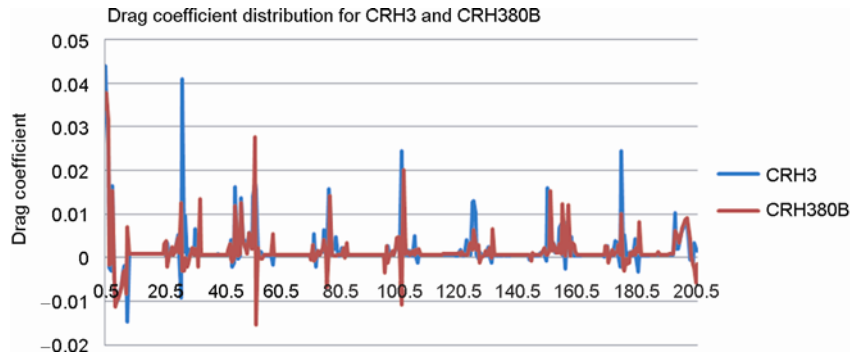
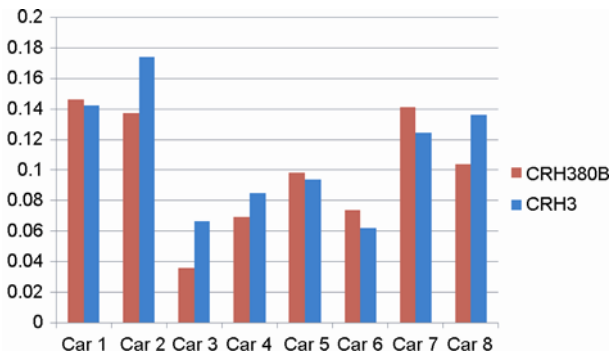**Figure 16**   Aerodynamic drag distributions for CRH3 and CRH380B.

Figure 17   Aerodynamic drag distribution of cars.

Table 1   The effects of drag deduction

Model	Modification description	Drag
1	Adding half outer joint parts between two cars	−4.1%
2	Adding full outer joint parts between two cars	−4.2%
3	Streamline ventilation covers	−1.4%
4	Streamline pantograph covers and without ventilation covers	−4.6%
5	Adding 80 mm skirts for all bogie region	−0.9%
6	5+only half skirt for first bogie region	−1.7%
7	5+only full wrapping skirt for first bogie	−5.7%
8	1+3+5+streamline pantograph covers	−8.9%

deductions of CRH380B are on the second-car, the third-car, the fourth-car and the eighth-car, however, the drag augmentations are on the corresponding cars of the seventh-car, the sixth-car, the fifth-car and the first-car. The second-car with pantograph and its adjacent third-car, along with train-tail have obviously the effect on drag deduction. The decreased values of these cars are larger than the increased values of the corresponding anti-symmetric cars. The total aerodynamic drag of CRH380B decreases 8.67% with respect to the original train of CRH3. The target of drag deduction is achieved.

4   Conclusions

By numerical simulations and wind-tunnel tests, the new generation of high-speed train of CRH380A were determined based on aerodynamic performances from 20 train-head models designed under the consideration of geometrical variables and engineering limitation conditions. The running CRH380A train in the Beijing-Shanghai line testified that it has excellent aerodynamic performance.

By analyses of aerodynamic drag distributions of CRH3, the train parts of drag deduction were found. Through wind-tunnel tests, the local optimized structures for drag reduction were validated. Then the effect of drag deduction on the real train of CRH380B with eight-cars was calculated and compared with the original train of CRH3. The running CRH380B train in the Beijing-Shanghai line also showed that it has excellent aerodynamic performance.

1   Raghu S, Raghunathan H, Kim D, et al. Aerodynamics of high-speed railway train. Prog Aerosp Sci, 2002, 38: 469–514

2   Joseph A, Schetz. Aerodynamics of high-speed trains. Ann Rev Fluid Mech, 2001, 33: 371–414

3   Sun Z X, Song J J, An Y R. Optimization of the head shape of the CRH3 high speed train. Sci China Tech Sci, 2010, 12: 3356–3364

4   Lee J S, Kim J H. Approximate optimization of high-speed train nose shape for reducing micropressure wave. Ind Appl, 2008, 35: 79–87

5   Kwon H B, Jang K H, Kim Y S. Nose shape optimization of high-speed train for minimization of tunnel sonic boom. Japan Soc Mech Eng, 2001, 4: 890–899

6   Zheng G N, Deng S C, Han T L, et al. The investigation on parallel implicit algorithm based on hybrid grid Navier-Stokes equations (in Chinese). Chin J Appl Mech, 2011, 28(3): 211–218